Editors' Suggestion

Water-Mediated Protein-Protein Interactions at High Pressures are Controlled by a Deep-Sea Osmolyte

Karin Julius,[1] Jonathan Weine,[1] Melanie Berghaus,[2] Nico König,[1] Mimi Gao,[2] Jan Latarius,[1] Michael Paulus,[1] Martin A. Schroer,[3] Metin Tolan,[1] and Roland Winter[2]
[1]*Faculty of Physics/DELTA, TU Dortmund University, 44221 Dortmund, Germany*
[2]*Faculty of Chemistry and Chemical Biology, TU Dortmund University, Otto-Hahn-Strasse 4a, 44227 Dortmund, Germany*
[3]*European Molecular Biology Laboratory (EMBL) Hamburg c/o DESY, Notkestrasse 85, 22607 Hamburg, Germany*

(Received 22 February 2018; published 16 July 2018)

The influence of natural cosolvent mixtures on the pressure-dependent structure and protein-protein interaction potential of dense protein solutions is studied and analyzed using small-angle X-ray scattering in combination with a liquid-state theoretical approach. The deep-sea osmolyte trimethylamine-*N*-oxide is shown to play a crucial and singular role in its ability to not only guarantee sustainability of the native protein's folded state under harsh environmental conditions, but it also controls water-mediated intermolecular interactions at high pressure, thereby preventing contact formation and hence aggregation of proteins.

DOI: 10.1103/PhysRevLett.121.038101

Cosolvents or osmolytes, such as free amino acids, methylamines, sugars, and polyols as well as the denaturant urea (Fig. 1) can be accumulated to rather high concentrations by cells. They adjust cell volume and osmotic pressure to harsh extracellular environments, such as high temperature, freezing, and anhydrobiosis or to high hydrostatic pressure as encountered in the deep sea up to the 1 kbar level [1]. Sugars and polyols are dominantly accumulated by organisms to increase thermostability, as are trehalose and proline to protect membranes from freezing. Methylamines are able to counteract salt and urea inhibition of enzymes [2]. Trimethylamine-*N*-oxide (TMAO) is known to counteract temperature- and pressure-induced destabilization of proteins [3–6]. Previous studies have shown that a repulsion between stabilizing agents such as TMAO and the peptide-bond backbone of proteins results in a strong exclusion of the cosolvent from the protein surface (depending on the protein charge [7–9]) and hence in preferential hydration of the protein surface. Reducing the exposure of hydrated surface area and thus the entropically unfavorable interaction between cosolvent and protein backbone stabilizes native protein folds against denaturation [7,10]. In contrast, perturbants such as urea are accumulated at the protein surface and destabilize proteins at high concentrations, interacting favorably with the protein backbone and amino acid side chains [7,10].

In nature, mixtures of counteracting osmolytes are often found to be more beneficial to cells than single ones. Correlating with habitat depth and thus hydrostatic pressure, significant differences in the osmolyte compositions of cellular fluids (e.g., in shrimps, skates, and crabs) compared to their shallow-living relatives are reported. The highest levels of methylamines, especially TMAO, are accumulated under abyssal environments [3,11]. The mechanisms of protein stabilization and, in particular, the linkage to the intermolecular interactions between proteins in such cosolvent mixtures at ambient as well as at elevated pressure are still largely *terra incognita*.

Here, we focus on the impact of different biologically relevant cosolvent mixtures on the pressure-dependent intermolecular pair interaction potential $V(r)$ of highly concentrated protein solutions (mimicking cell-like crowding conditions), applying small-angle x-ray scattering (SAXS) and liquid-state theoretical approaches. To probe protein-protein interactions in such cosolvent solutions, the protein lysozyme is employed, which is conformationally stable up to 5 kbar and has been used before for this purpose [4,12]. Changes of the interaction potential have also been shown to impact on the macroscopic phase behavior of dense protein solutions, such as the liquid-liquid phase separation region, where the homogeneous protein solution separates into two coexisting liquid phases of different protein concentration, a scenario being considered to be of high relevance to the biophysics of cells. A reentrant liquid-liquid phase coexistence region has been found at elevated pressures [13]. By focusing on osmolyte mixtures mimicking cellular fluids encountered in deep-sea organisms, such as shallow- and deep-living crabs, skates, and shrimps (see Fig. 1 and SI of the Supplemental Material [14]), we are able to go one step further towards a better understanding of "real" biological intracellular fluids as they appear in nature and reveal details and differential effects of their protecting properties.

The SAXS intensity $I(q)$ of a solution of interacting globular particles such as lysozyme molecules is described by

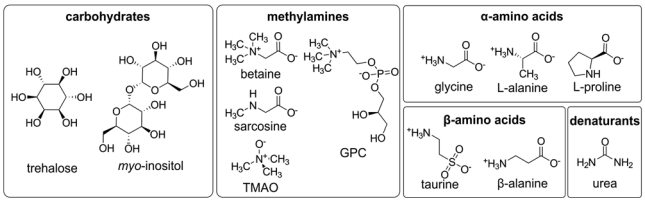

FIG. 1. Structure of α and β amino acids, the denaturant urea, carbohydrates, and methylamines present as osmolytes in marine organisms. GPC = L-α-glycerophosphorylcholine.

$$I(q) \propto n_p \Delta\rho^2 V_p^2 \langle P(q)\rangle S_{\mathrm{eff}}(q), \tag{1}$$

where n_p is the average number density of particles in the sample, which is related to the protein's volume fraction Φ, V_p is the particle volume, and $\Delta\rho$ is the electron density contrast. The form factor $\langle P(q)\rangle$ describes the scattering of the single lysozyme molecule averaged over its orientation [36]. The effective structure factor $S_{\mathrm{eff}}(q)$ describes the spatial arrangement of the lysozyme molecules and is linked to the effective intermolecular interaction potential within the mean-spherical approximation (see SI of the Supplemental Material for details [14]) [36,37]. The position $q_{\max}$ of the correlation peak of $S_{\mathrm{eff}}(q)$ can be linked to the mean distance $d_{\mathrm{lys}} \approx 2\pi/q_{\max}$ between neighboring protein molecules.

The effective pair interaction potential of the lysozyme molecules in solution can be described by the Derjaguin-Landau-Verwey-Overbeek (DLVO) potential $V(r)$ [12,36]. It consists of the sum of a hard-sphere part $V_{\mathrm{HS}}(r)$, a long-ranged repulsive screened Coulomb part $V_{\mathrm{SC}}(r)$, and a short-ranged attractive Yukawian-like potential $V_{\mathrm{Y}}(r)$. To determine the structure factor theoretically, the DLVO potential is fitted to the scattering intensity $I(q)$. The single contributions to $V(r)$ are given by

$$\begin{aligned} V_{\mathrm{HS}}(r) &= \begin{cases} \infty, & r \le \sigma \\ 0, & r > \sigma, \end{cases} \\ V_{\mathrm{SC}}(r) &= \begin{cases} 0, & r \le \sigma \\ \frac{Z^2 e^2}{4\pi\varepsilon_0\varepsilon_r(1+0.5\kappa\sigma)^2}\frac{e^{-\kappa(r-\sigma)}}{r}, & r > \sigma, \end{cases} \\ V_{\mathrm{Y}}(r) &= \begin{cases} 0, & r \le \sigma \\ -J\sigma\frac{e^{-(r-\sigma/d)}}{r}, & r > \sigma, \end{cases} \end{aligned} \tag{2}$$

where ε_0 is the dielectric permittivity of the vacuum, ε_r is the static relative dielectric permittivity of the solvent, κ is the Debye-Hückel screening length, e is the elementary charge, and σ is the protein's effective hard-sphere diameter. The pressure dependence of ε_r of the aqueous solutions can be reasonably described by the pressure dependence of ε_r of water [38], taking into account the osmolytes' dielectric increments from the literature and from our own measurements (see Fig. SI 1 of the Supplemental Material [14]). For the width of the Yukawian potential, we chose $d = 0.3$ nm [12,36]. The effective net charge of the protein at pH 7 was set to $Z = +8e$ [39], which is essentially unchanged for all solution conditions studied (see SI of the Supplemental Material [14]). The only free parameter in the modeling of the experimental data remains the strength of the attractive part of the interaction potential J. The protein-protein osmotic second virial coefficient B_2 is a direct measure of the overall pair interaction potential and has been calculated from the DLVO potential parameters via [12,40]

$$B_2 = 2\pi \int_0^\infty \left[1 - \exp\left(-\frac{V(r)}{k_B T}\right)\right] r^2 dr. \tag{3}$$

The normalized second virial coefficient $b_2 = B_2/B_2^{\mathrm{HS}}$ is obtained by factoring out the contribution of the hard-sphere part of the integral B_2^{HS} [41]; b_2 is positive for predominantly repulsive interactions and negative for attraction. Figure 2 exemplifies the data analysis procedure for the experimental SAXS intensities $I(q)$ of 10% (w/v) lysozyme in 25 mM bis-tris (pH 7) buffer as a function of trehalose concentration c and pressure p at $T = 25\,^{\circ}\mathrm{C}$.

A pronounced intermolecular correlation peak is observed at momentum transfer q_{corr}, indicating a repulsive

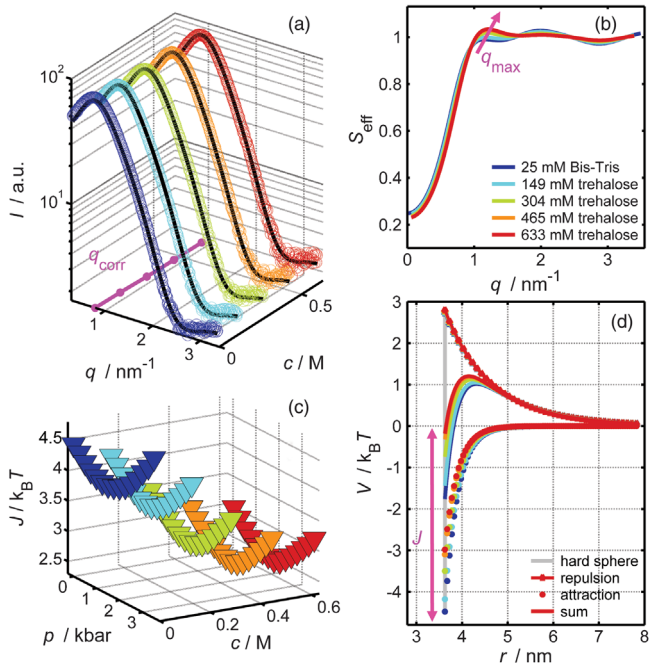

FIG. 2. (a) Experimental SAXS data $I(q)$ for a 10% (w/v) lysozyme in 25 mM Bis-Tris solution at 25 °C and 1 bar for various trehalose concentrations c. Black lines display the refinement of the data. (b) Results of the refinement for the effective structure factor $S_{\mathrm{eff}}(q)$ at various trehalose concentrations. (c) Strength of the attractive interaction $J(c, p)$ as a function of trehalose concentration c and pressure p. (d) Total protein-protein interaction potential $V(r)$ (sum) displayed together with its contributing parts.

short-range ordering of the lysozyme molecules, which shifts towards higher q values with increasing trehalose concentration [Fig. 2(a)]. Division of the scattering intensities by the analytical form factor, obtained from the refinement of the scattering pattern of a dilute lysozyme solution, yields the effective structure factor $S_{\mathrm{eff}}(q)$. The refinements of $S_{\mathrm{eff}}(q)$ to extract the effective protein-protein interaction potential $V(r)$ are displayed in Fig. 2(a) as solid black lines. The first maximum of $S_{\mathrm{eff}}(q)$ shifts with the increasing trehalose concentration to slightly higher q values, and its height increases concomitantly. The increase of q_{max} corresponds to a slight decrease of the mean intermolecular spacing between adjacent lysozyme molecules d_{lys}. The resulting DLVO effective pair interaction potential is depicted together with its individual contributions in Fig. 2(d). In calculating the repulsive (screened) Coulomb contribution, the decrease in dielectric permittivity upon addition of trehalose ($d\varepsilon_r/dc = 7.53\ \mathrm{M}^{-1}$) was taken into account, which leads to an increase in the long-range repulsive interaction $V_{\mathrm{SC}}(r)$ and a concomitant decrease in the depth of the attractive part of $V(r)$, J [Fig. 2(c)]. Nonetheless, a slight decrease of d_{lys} is observed. Such an effect might be rationalized invoking an excluded volume effect imposed by the compatible cosolvent.

To reveal potential pressure-dependent changes in the structure of the lysozyme molecule, SAXS measurements were carried out on diluted 1% (w/v) ($\sim$10 mg mL^{-1}) lysozyme solutions in a pressure range from 1 to 3500 bar for all solution conditions. A constant radius of gyration of $R_G = 1.45 \pm 0.02$ nm was found for all cosolvents studied, indicating that the protein remained in its folded state in the whole pressure range covered (see Fig. SI 7 of the Supplemental Material [14]). Subsequently, pressure-dependent measurements on the 10% (w/v) ($\sim$102.7 mg mL^{-1}) lysozyme solution were performed to reveal changes in the intermolecular interaction by combined pressure-cosolvent effects. First, a monotonic decrease of J is visible in comparison to the pure buffer system with increasing trehalose concentration [Fig. 2(c)]. Second, the nonmonotonic pressure dependence of $J(p)$, as found in previous studies on the pure dense lysozyme solution [36], persists at all cosolvent concentrations. As the solution is continuously compressed, the intermolecular spacing d_{lys} is slightly reduced and $V(r)$ is affected by a decrease of J. Remarkably, upon a pressure increase beyond $\sim$1.6 kbar, this effect is reversed. Such a trend reversal has been proposed to be due to a change of the bulk water structure upon pressurization [42,43].

To explore the effects of the single cosolvents on $V(r)$ systematically, corresponding measurements were carried out for all of them, covering the whole concentration range from 0 to 1 M. Figure 3 displays the J and b_2 data dependence of cosolvent concentration and pressure. Clearly, a marked cosolvent concentration dependence of

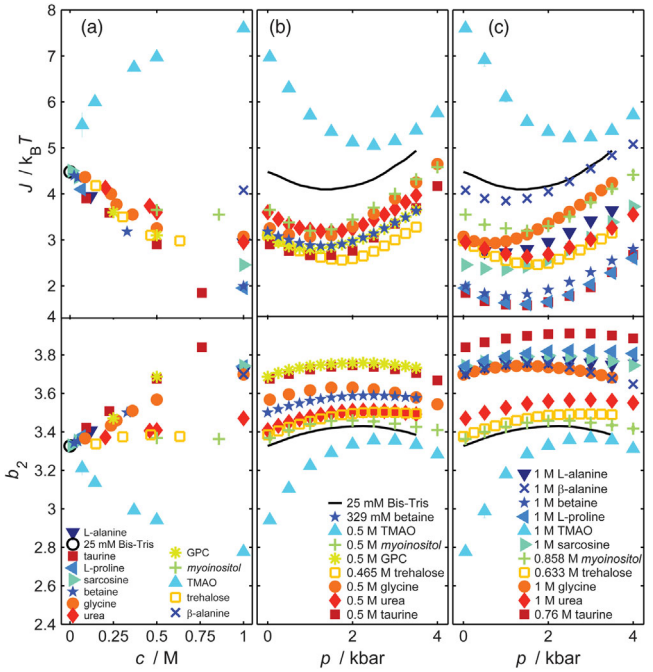

FIG. 3. (a) Results of the refinement for the strength of the attractive part J and the normalized second virial coefficient b_2 as a function of osmolyte concentration c (in M = mol L^{-1}), at 25 °C and ambient pressure, and as a function of pressure for midlevel (b) and highest (c) osmolyte concentrations. For comparison, the pure buffer system is depicted as well (black circle, solid line).

the potential parameters is visible, in particular at high concentrations. Two distinct cosolvent classes with contrasting effects on $J(c)$ and $b_2(c)$ emerge: one class is solely formed by TMAO, and the second class comprises all other cosolvents. In agreement with data from the literature [4], TMAO distinctly increases the attractive part of the lysozyme's pair interaction potential. Remarkably, the other cosolvents, even though of disparate chemical makeup, render the overall pair interaction potential more repulsive; i.e., J decreases in a linear way with increasing osmolyte concentration. Differences become visible at higher cosolvent concentrations, only, i.e., in the region where changes in dielectric solution properties become more prominent.

The static dielectric increments $\delta = d\varepsilon_r/dc$ of the cosolvents in aqueous solution can be placed in the order $\delta(\mathrm{trehalose}) = -7.53\ \mathrm{M}^{-1} <$ *myo*-inositol (negative) $<$ water $<$ (positive) urea $\sim$ TMAO $<<$ betaine $<$ L-proline $<$ glycine $\sim$ L-alanine $\sim$ sarcosine $<<$ β-alanine $<$ taurine $\sim\delta(\mathrm{GPC}) = +43.8\ \mathrm{M}^{-1}$ (Fig. SI 1 of the Supplemental Material [14]). The increase of ε_r with increasing osmolyte concentration is strongest for taurine and GPC, which should lead to stronger screening and hence a reduction of Coulomb repulsion. As seen by the strong increase of b_2 with c, this does not seem to be the case. Rather, $J(c)$ exhibits a strong negative gradient, indicating increasing repulsion. Hence, again, an excluded volume effect seems

to dominate over electrostatics, which leads to a slight decrease of d_{lys}.

A completely different scenario is observed for TMAO, which changes ε_r, similar to urea, only very little ($\delta = +2.16\ \mathrm{M}^{-1}$). Different from all other cosolvents, even 0.5 M TMAO leads to a drastic increase of the attractivity, i.e., J. Such a strong increase of J must have some other origin. Strong differences in $J(c)$ and $b_2(c)$ might be accounted for by a modification of the van der Waals potential contributing to the attractive Yukawian part of the DLVO potential via solvent-induced changes of the Hamaker constant A. Calculation of A for all solution conditions (Fig. SI 4 of the Supplemental Material [14]) reveals that the least attractive interaction should be observed in trehalose and the strongest in urea and TMAO. Such a scenario is not observed in the experimental data showing strong attractive interaction for TMAO only [Fig. 3(a)]. Hence, solvent-induced changes of the Hamaker constant are not able to explain the particular behavior of TMAO.

The impact of the Coulomb repulsion on $V(r)$ should become significant upon compression owing to a decrease of interatomic spacings and the monotonic increase of ε_r with pressure [38]. As shown in Figs. 3(b), (c), a decrease in J and a concomitant increase of b_2 is in fact observed upon compression. However, this effect is noticeable up to ~1.6 kbar only, where a trend reversal emerges. Remarkably, addition of all the osmolytes leads to a modulation of the $J(p)$ and $b_2(p)$ curves only, but leaves their general shape essentially unchanged; i.e., the underlying mechanism of this effect ought to be universal. Next to 1 M glycine, significant differences are found for TMAO only, which entails a much stronger pressure dependence and a shift of the minimum in $J(p)$ and maximum of $b_2(p)$ to ~1 kbar higher pressures (Figs. 3, SI 5 of the Supplemental Material [14]). Such an effect may be due to significant structural changes of the solvent and/or to a very strong thermodynamically favored exclusion of the additive from the protein surface, i.e., a strong solvophobic effect, which decreases intermolecular distances and apparently increases intermolecular attractive interactions.

In a next step, high-pressure SAXS data were taken on 10% (w/v) lysozyme solutions consisting of cosolvent mixtures mimicking conditions encountered in deep-sea organisms, such as shallow- and deep-living crabs, skates, and shrimps [11] (see SI of the Supplemental Material [14]). Remarkably, for all species, their TMAO content rises with the increasing ocean depth, i.e., hydrostatic pressure. Figure 4 displays the corresponding potential parameter $J(p)$ together with data of the main contributing osmolytes of deep (bathyal and abyssal)-living and shallow-living species. The data unambiguously show that the cosolvents other than TMAO are largely interchangeable. Moreover, their effect is to weaken the impact of TMAO, depending on the cosolute structure to different extents,

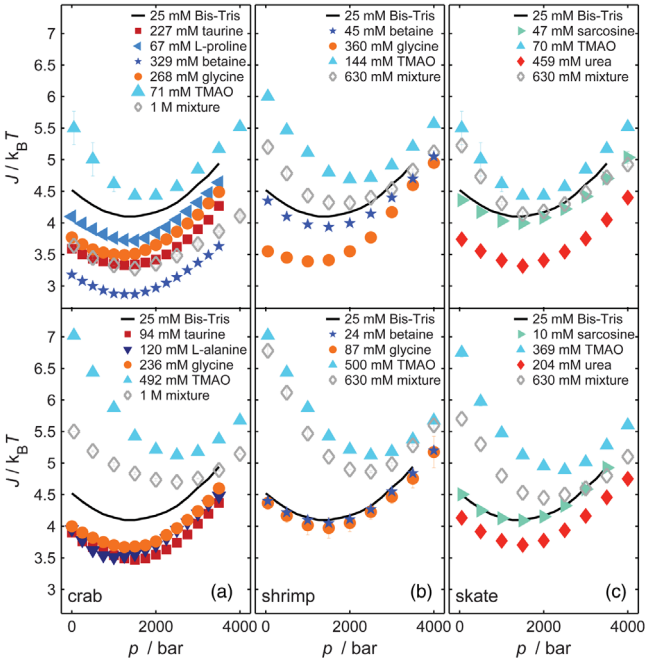

FIG. 4. Pressure dependence of the strength of the attractive protein-protein interaction J in 10% (w/v) lysozyme +25 mM Bis-Tris (pH 7) at 25 °C with osmolyte mixtures added as found for shallow-living (top half) and deep-living (bottom half) crabs (a), shrimps (b), and skates (c) [11]. The results for the pure buffer (solid black line) and for the contributing single cosolvent solutions are shown as well.

however. Consequently, the marked effect of TMAO on the potential parameters is reduced and the shift of the minimum in $J(p)$ to higher pressures is reversed, not only by the denaturant urea, but also by the presence of the other cosolvents (as exemplarily demonstrated for glycine in Fig. SI 5 of the Supplemental Material [14]).

As TMAO is also known to stabilize proteins and other biomolecules most effectively [7], it appears that natural osmolyte mixtures are assembled in such a way that an overstabilization and too strong attractivity induced by TMAO is compensated, which might be needed to preserve normal cellular functionality. The peculiar role TMAO is playing is clearly evident and might be due to its ability to counteract pressure effects by strengthening and increasing the amount of water-water hydrogen bonds as well as by a strong spatial ordering of the solution's hydrogen bond network [7,44].

Seeking to reveal an additional proof for such a water-mediated effect, information on many-body structural correlations is expected to be helpful. For describing hydrogen-bonded liquids, such as water itself or protein solutions, next to two-body, triplet correlation functions (TCFs) also seem to play a prominent role [45–47]. Such information can be obtained through measurements of the pressure derivative of the effective structure factor $[\partial S_{\mathrm{eff}}(q)/\partial p]_T$ (see SI of the Supplemental Material for

details [14]). As shown in Figure SI 6, the 0.5 M TMAO solution reveals significant changes in the TCF from the other cosolvent solutions. Further, changes in the shape of $[\partial S_{\mathrm{eff}}(q)/\partial p]_T$ and hence in the TCF are moved to ~1 kbar higher pressures, elucidating that the water-mediated protein-protein interaction potential is significantly different in the TMAO solution.

To conclude, at conditions where intermolecular distances between proteins reach values of a few water layers only (i.e., under cell-like crowding conditions), a change in the second coordination shell of water and increased hydration repulsion between lysozyme molecules seem to lead to the reversal of attractive interaction and intermolecular spacing upon compression. Changes in cosolvent-water interactions—such as an inward shift of the pair correlation function of oxygen atoms in water $g_{OwOw}(r)$ by TMAO [48]; a cross-interaction between cosolvents, such as that of TMAO and urea observed at ambient pressure [49,50]; or changes in protein-cosolvent-water interactions—may modulate this behavior.

Natural cosolvents are able to modulate the protein-protein interaction potential and its pressure dependence to variable extents. Addition of the deep-sea osmolyte TMAO leads to a pronounced excluded volume and affects $V(r)$ most strongly, owing to its particular structure, being a small solute that offers both strongly hydrophilic and hydrophobic solvation regions and its strong dipole moment (~5 D) and H-bonding capability as well as repulsive self-interaction [8]. The other cosolutes seem to function essentially as osmoregulators only. TMAO not only guarantees sustainability of the native protein's folded state under harsh environmental conditions [3–6], it also controls water-mediated intermolecular interactions at high pressure, thereby preventing contact formation and hence aggregation of proteins. Embedded Cluster Reference Interaction Site Model (EC-RISM) theory in concert with *ab initio* molecular dynamics simulations and FTIR data have recently revealed a charge redistribution upon compression of TMAO, and it has been suggested that the key ingredient to high-pressure adaption might be an increased solvent-induced polarization and locally enhanced H-bonding network [51,52].

The authors kindly acknowledge ESRF, DLS, DELTA, and SOLEIL for providing synchrotron radiation and J. Möller (ID02), A. Smith (I22), R. Wagner (BL8), and J. Perez (SWING) for technical support. We thank C. Gainaru for technical support during the dielectric measurements. This Letter was financially supported by the Cluster of Excellence RESOLV (EXC 1069) funded by the DFG.

[1] P. W. Hochachka and G. N. Somero, *Biochemical Adaptation* (Oxford University Press, Oxford, New York 2002).
[2] P. H. Yancey, J. Exp. Biol. **208**, 2819 (2005).
[3] P. H. Yancey, A. L. Fyfe-Johnson, R. H. Kelly, V. P. Walker, and M. T. Auñón, J. Exp. Zool. **289**, 172 (2001).
[4] M. A. Schroer, Y. Zhai, D. C. F. Wieland, C. J. Sahle, J. Nase, M. Paulus, M. Tolan, and R. Winter, Angew. Chem., Int. Ed. **50**, 11413 (2011).
[5] M. Gao, C. Held, S. Patra, L. Arna, G. Sadowski, and R. Winter, Chem. Phys. Chem. **18**, 2951 (2017).
[6] T. Arakawa and S. N. Timasheff, Biophys. J. **47**, 411 (1985).
[7] D. R. Canchi and A. E. García, Annu. Rev. Phys. Chem. **64**, 273 (2013).
[8] D. R. Canchi, P. Jayasimha, D. C. Rau, G. I. Makhatadze, and A. E. García, J. Phys. Chem. B **116**, 12095 (2012).
[9] Z. Su, F. Mahmoudinobar, and C. L. Dias, Phys. Rev. Lett. **119**, 108102 (2017).
[10] S. N. Timasheff and G. Xie, Biophys. Chem. **105**, 421 (2003).
[11] R. H. Kelly and P. H. Yancey, Biol. Bull. **196**, 18 (1999).
[12] J. Möller, M. A. Schroer, M. Erlkamp, S. Grobelny, M. Paulus, S. Tiemeyer, F. J. Wirkert, M Tolan, and R. Winter, Biophys. J. **102**, 2641 (2012).
[13] J. Möller, S. Grobelny, J. Schulze, S. Bieder, A. Steffen, M. Erlkamp, M. Paulus, M. Tolan, and R. Winter, Phys. Rev. Lett. **112**, 028101 (2014).
[14] See Supplementary Material at http://link.aps.org/supplemental/10.1103/PhysRevLett.121.038101 for additional figures and more details on the materials, experimental methods, and analysis of the small-angle x-ray scattering data. The Supplementary Material includes Refs. [15–35].
[15] C. Krywka, C. Sternemann, M. Paulus, M. Tolan, C. Royer, and R. Winter, Chem. Phys. Chem. **9**, 2809 (2008).
[16] M. Kotlarchyk and S. H. Chen, J. Chem. Phys. **79**, 2461 (1983).
[17] F. J. Millero, G. K. Ward, and P. Chetirkin, J. Biol. Chem. **251**, 4001 (1976).
[18] *Topics in Current Chemistry 111*, Physical and Inorganic Chemistry, edited by J. Barthel (Springer, Berlin, 1983).
[19] J. Barthel, K. Bachhuber, R. Buchner, and H. Hetzenauer, Chem. Phys. Lett. **165**, 369 (1990).
[20] U. Kaatze and V. Uhlendorf, Z. Phys. Chem. **126**, 151 (1981).
[21] J. Wyman, Jr. and T. L. McMeekin, J. Am. Chem. Soc. **55**, 908 (1933).
[22] E. J. Cohn and J. T. Edsall, *Proteins, Amino Acids and Peptides* (Hafner, New York, 1965).
[23] J. T. Edsall and J. Wyman, Jr., J. Am. Chem. Soc. **57**, 1964 (1935).
[24] F. Franks, D. S. Reid, and A. Suggett, J. Solution Chem. **2**, 99 (1973).
[25] J. Hunger, K. J. Tielrooij, R. Buchner, M. Bonn, and H. J. Bakker, J. Phys. Chem. B **116**, 4783 (2012).
[26] M. Sajadi, Y. Ajaj, I. Ioffe, H. Weingärtner, and N. P. Ernsting, Angew. Chem., Int. Ed. **49**, 454 (2010).
[27] J. Wyman, Chem. Rev. **19**, 213 (1936).
[28] R. J. Hunter, *Foundations of Colloid Science* (Oxford University Press, Oxford, New York, 2004).
[29] J. N. Israelachvili, *Intermolecular and Surface Forces* (Academic Press, Burlington (2011).
[30] J. J. Dwyer, A. G. Gittis, D. A. Karp, E. E. Lattman, D. S. Spencer, W. E. Stites, and E. B. García-Moreno, Biophys. J. **79**, 1610 (2000).

[31] M. Farnum and C. Zukoski, Biophys. J. **76**, 2716 (1999).
[32] D. L. Rickard, P. B. Duncan, and D. Needham, Biophys. J. **98**, 1075 (2010).
[33] P. H. Yancey, W. R. Blake, and J. Conley, Comp. Biochem. Physiol., Part A, Mol. Integr. Physiol. **133**, 667 (2002).
[34] D. I. Svergun, A. V. Semenyuk, and L. A. Feigin, Acta Crystallogr. Sect. A **44**, 244 (1988).
[35] D. I. Svergun, J. Appl. Crystallogr. **25**, 495 (1992).
[36] M. A. Schroer, J. Markgraf, D. C. F. Wieland, C. J. Sahle, J. Möller, M. Paulus, M. Tolan, and R. Winter, Phys. Rev. Lett. **106**, 178102 (2011).
[37] Y. Liu, W. R. Chen, and S. H. Chen, J. Chem. Phys. **122**, 044507 (2005).
[38] W. B. Floriano and M. A. C. Nascimento, Braz. J. Phys. **34**, 38 (2004).
[39] D. E. Kuehner, J. Engmann, F. Fergg, M. Wernick, H. W. Blanch, and J. M. Prausnitz, J. Phys. Chem. B **103**, 1368 (1999).
[40] J. Narayanan and X. Y. Liu, Biophys. J. **84**, 523 (2003).
[41] H. Sedgwick, J. E. Cameron, W. C. K. Poon, and S. U. Egelhaaf, J. Chem. Phys. **127**, 125102 (2007).
[42] A. K. Soper and M. A. Ricci, Phys. Rev. Lett. **84**, 2881 (2000).
[43] Y. Katayama, T. Hattori, H. Saitoh, T. Ikeda, K. Aoki, H. Fukui, and K. Funakoshi, Phys. Rev. B **81**, 014109 (2010).
[44] Q. Zou, B. J. Bennion, V. Daggett, and K. P. Murphy, J. Am. Chem. Soc. **124**, 1192 (2002).
[45] D. Dhabal, K. T. Wikfeldt, L. B. Skinner, C. Chakravarty, and H. K. Kashyap, Phys. Chem. Chem. Phys. **19**, 3265 (2017).
[46] P. A. Egelstaff, D. I. Page, and C. R. T. Heard, J. Phys. C **4**, 1453 (1971).
[47] M. A. Schroer, M. Tolan, and R. Winter, Phys. Chem. Chem. Phys. **14**, 9486 (2012).
[48] J. J. Towey, A. K. Soper, and L. Dougan, Faraday Discuss. **167**, 159 (2013).
[49] P. Ganguly, T. Hajari, J.-E. Shea, and N. F. A. van der Vegt, Phys. Chem. Lett. **6**, 581 (2015).
[50] J. Hunger, N. Ottosson, K. Mazur, M. Bonn, and H. J. Bakker, Phys. Chem. Chem. Phys. **17**, 298 (2015).
[51] C. Hölzl, P Kibies, S. Imoto, R. Frach, S. Suladze, R. Winter, D. Marx, D. Horinek, and S. M. Kast, J. Chem. Phys. **144**, 144104 (2016).
[52] S. Imoto, P. Kibies, C. Rosin, R. Winter, S. M. Kast, and D. Marx, Angew. Chem., Int. Ed. **55**, 9534 (2016).